

Synthesis of TiC via polymeric titanates: the preparation of fibres and thin films

K. THORNE, S. J. TING, C. J. CHU, J. D. MACKENZIE, T. D. GETMAN*, M. F. HAWTHORNE*

*Department of Materials Science and Engineering, and *Department of Chemistry and Biochemistry, University College of Los Angeles, Los Angeles, CA 90024, USA*

Polymerization of titanium isopropoxide via its transesterification with *o*-xylene- α,α' -diacetate enables the formation of a polymeric titanate that can be thermally converted into carbon-deficient TiC after inert atmosphere pyrolysis at 800 °C. The physical and rheological properties of this polymeric titanate allow for the production of crystalline TiC fibres and thin films. The synthesis of this polymeric precursor and the structural transformations leading to the formation of TiC are discussed.

1. Introduction

The physical and electrical properties of TiC are ideal for numerous high-temperature applications [1, 2]. Unfortunately, the techniques currently used for the production of TiC have restricted its use in these applications. In fact, the current production techniques are physically and economically limited to the formation of chemical vapour deposited (CVD) films and sintered TiC ceramics [3, 4]. In order to exploit the advantages of TiC, alternative techniques for its fabrication must be developed.

Recently, the preparation of non-oxide ceramics through the pyrolysis of polymeric precursors has attracted much attention [5–8]. The use of polymeric precursors offers several unique advantages that can include lower processing temperatures, improved product purities and homogeneities and the ability to form fibres and thin films. In this report, these advantages have been exploited for the preparation of TiC fibres and films.

Bulk titanium carbide is generally prepared by the carbothermal reduction of titania [5, 6]. As compared to traditional solid state reactions, polymeric precursors made from titanium alkoxides are better suited for the preparation of TiC as they can provide an intimate, molecular scale mixture of titania and carbon. Furthermore, the rheological properties of the polymeric precursors can be controlled to enable the formation of fibres and films. Early attempts using such polymeric precursors showed that it is relatively simple to prepare crystalline TiC powders [9]. However, the fabrication of TiC fibres has proved to be difficult.

To prepare a polymer precursor appropriate for the production of TiC fibres, polymerization of titanium isopropoxide via transesterification with bifunctional acetates, $\text{H}_3\text{CCOO-R-OOCCH}_3$ [$\text{R}=(\text{CH}_2)_3$, $(\text{CH}_2)_4$, *m*-xylene, *o*-xylene, *p*-xylene], was employed [9]. This approach eliminates certain processing problems inherent in the typically used sol-gel polymer-

izations [10, 11]. In addition, the proper choice and use of different organic (R) groups could enable control of both the internal carbon concentration and the rheological properties of the resultant polymers.

In this work, studies were conducted using polymeric titanates prepared by the transesterification of titanium isopropoxide [$\text{Ti}(\text{O-}i\text{-C}_3\text{H}_7)_4$] according to the reactions listed in Table I. The products were preliminarily screened based upon: (1) solubility, (2) ability to be drawn into fibres, (3) ability to form TiC, and (4) the temperature at which TiC formed. Transesterification of titanium isopropoxide with *o*-xylene- α,α' -diacetate results in a polymeric titanate that is soluble in common solvents, can be easily drawn into fibres and yields carbon-deficient TiC upon pyrolysis at 800 °C. The synthesis, characterization and conversion of this polymeric precursor into TiC is described below.

2. Experimental procedure

All manipulations of the titanates were carried out either in an inert atmosphere glove box or by means of standard Schlenk techniques. Titanium(IV) isopropoxide and 1,2-benzene-dimethanol were purchased and used without further purification. Toluene was distilled from sodium and degassed immediately before use and deuterated chloroform was dried over P_2O_5 , distilled and stored in the glove box.

^1H NMR spectra were recorded with a Bruker AF-200 (200.132 MHz)–Fourier transform–nuclear magnetic resonance (FT–NMR) spectrometer. ^{13}C NMR spectra were recorded using a Bruker AM-360 (90.556 MHz) FT–NMR spectrometer. Solid state ^{13}C cold plasma–magic angle spinning–NMR (CP–MAS–NMR) spectra were recorded with a Bruker MSL-300 (75.470 MHz) FT–NMR spectrometer using a relaxation delay of 8.0 s and a pulse width of 10.0 μs . The CP–MAS–NMR samples were spun at approximately 4000 Hz. Transmission infrared spectra were obtained using either a Perkin

TABLE I Summary of the reactions of various esters with titanium isopropoxide $[\text{Ti}(\text{O}-i\text{-C}_3\text{H}_7)_4]$

Acetate	Ratio	Theoretical polymer structure	Solubility	Temperature at which TiC_x was formed ($^\circ\text{C}$)
$\text{C}(\text{CH}_2\text{OCCH}_3)_4$	1:1	$\left\{ \begin{array}{c} \text{OCH}_2 \quad \text{CH}_2\text{O} \\ \diagdown \quad \diagup \\ \text{Ti} \quad \text{C} \\ \diagup \quad \diagdown \\ \text{OCH}_2 \quad \text{CH}_2\text{O} \end{array} \right\}_n$	Insoluble	1500
$\text{H}_3\text{CCO}-(\text{CH}_2)_3-\text{OCCH}_3$	2:1	$\left\{ \begin{array}{c} \text{O}-(\text{CH}_2)_3-\text{O} \\ \diagdown \quad \diagup \\ \text{Ti} \\ \diagup \quad \diagdown \\ \text{O}-(\text{CH}_2)_3-\text{O} \end{array} \right\}_n$	Insoluble	NA
$\text{H}_3\text{CCO}-(\text{CH}_2)_3-\text{OCCH}_3$	1:1	$\left\{ \begin{array}{c} -\text{Ti}-\text{O}-(\text{CH}_2)_3-\text{O}- \\ \\ (\text{O}-\text{CH}(\text{CH}_3)_2) \end{array} \right\}_n$	Soluble in toluene, benzene, hexane, and CH_2Cl_2	1600
$\text{H}_3\text{CCO}-(\text{CH}_2)_4-\text{OCCH}_3$	2:1	$\left\{ \begin{array}{c} \text{O}-(\text{CH}_2)_4-\text{O} \\ \diagdown \quad \diagup \\ \text{Ti} \\ \diagup \quad \diagdown \\ \text{O}-(\text{CH}_2)_4-\text{O} \end{array} \right\}_n$	Soluble in toluene, benzene, hexane, and CH_2Cl_2	No TiC TiO formed
$\text{H}_3\text{CCO}-\text{CH}_2-\text{C}_6\text{H}_4-\text{CH}_2-\text{OCCH}_3$	2:1	$\left\{ \begin{array}{c} \text{OCH}_2-\text{C}_6\text{H}_4-\text{CH}_2\text{O} \\ \diagdown \quad \diagup \\ \text{Ti} \\ \diagup \quad \diagdown \\ \text{OCH}_2-\text{C}_6\text{H}_4-\text{CH}_2\text{O} \end{array} \right\}_n$	Insoluble	1100
$\text{H}_3\text{CCO}-\text{CH}_2-\text{C}_6\text{H}_4-\text{CH}_2-\text{OCCH}_3$	1:1	$\left\{ \begin{array}{c} -\text{Ti}-\text{O}-\text{CH}_2-\text{C}_6\text{H}_4-\text{CH}_2-\text{O}- \\ \\ (\text{O}-\text{CH}(\text{CH}_3)_2) \end{array} \right\}_n$	Insoluble	1100
$\text{C}_6\text{H}_3(\text{CH}_2\text{OCCH}_3)_2$	1:1	$\left\{ \begin{array}{c} -\text{Ti}-\text{O}-\text{CH}_2-\text{C}_6\text{H}_3-\text{CH}_2-\text{O}- \\ \\ (\text{O}-\text{CH}(\text{CH}_3)_2) \end{array} \right\}_n$	Insoluble	1100
$\text{H}_3\text{CCO}-\text{CH}_2-\text{C}_6\text{H}_3(\text{CH}_2\text{OCCH}_3)_2$	1:1	$\left\{ \begin{array}{c} -\text{Ti}-\text{O}-\text{CH}_2-\text{C}_6\text{H}_3-\text{CH}_2-\text{O}- \\ \\ (\text{O}-\text{CH}(\text{CH}_3)_2) \end{array} \right\}_n$	Soluble in toluene, benzene, hexane, and CH_2Cl_2	800

Elmer 1330 photospectrometer over a range of $4000\text{--}200\text{ cm}^{-1}$ or a Beckman FT-1100 photospectrometer over a range of $4000\text{--}500\text{ cm}^{-1}$.

The differential thermal analysis (DTA) and the thermogravimetric analysis (TGA) results were obtained with a Perkin Elmer Thermostatation using models DTA 1600 and TGS-2. X-ray diffraction patterns were obtained with a Phillips diffractometer using $\text{CuK}\alpha_1$ radiation at 40 kV and 30 mA. Elemental analysis was conducted by Galbraith Laboratories, Knoxville, TN.

The polymeric titanates were pyrolysed at temperatures below $800\text{ }^\circ\text{C}$ in a refractory furnace operated inside a nitrogen atmosphere glove box. Pyrolysis at temperatures between 800 and $1500\text{ }^\circ\text{C}$ was conducted in a flowing argon atmosphere (99.999% Ar), graphite

refractory furnace (Thermal Technology – Series 1000). All samples were heated at a rate of approximately $10\text{ }^\circ\text{C min}^{-1}$.

2.1. Preparation of *o*-xylene- α,α' -diacetate

To 50.5 g (0.365 mol) 1,2-benzene dimethanol was added 150 ml acetic anhydride. The resulting solution was refluxed for 2.5 h. The solution was allowed to cool to room temperature and then added to 400 ml water. The aqueous solution was then extracted with three portions toluene (total volume 400 ml). Removal of the toluene on a rotary evaporator yielded a yellow oil. Distillation of the oil at $150\text{ }^\circ\text{C}$ under vacuum resulted in the isolation of 78.2 g (96%) of *o*-xylene- α,α' -diacetate as a white solid.

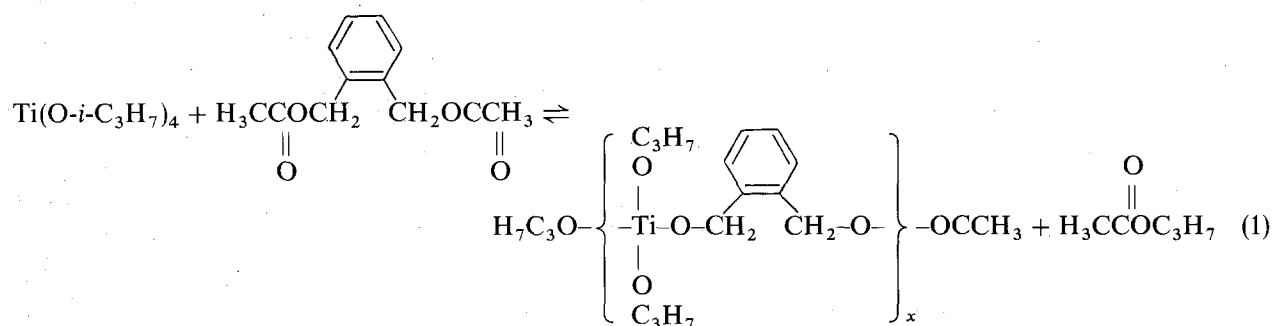
^1H NMR: 7.34 (m-aromatic H), 5.16 p.p.m. (s, CH_2), 2.06 p.p.m. (s), and 2.06 p.p.m. (s, CH_3): integration 2:2:3, respectively.

^{13}C NMR: 160.68 p.p.m., 134.54 p.p.m., 129.87 p.p.m., 128.77 p.p.m., 63.84 p.p.m., and 20.96 p.p.m.

Melting point: 36–37°C ($T_{\text{MP}} = 35^\circ\text{C}$ [12])

2.2. Reaction of $\text{Ti}(\text{O}-i\text{-C}_3\text{H}_7)_4$ with *o*-xylene- α,α' -diacetate

In a nitrogen atmosphere glove box, 7.036 g (25.38 mmol) titanium isopropoxide was weighed and quantitatively transferred, using 8 ml toluene, to a 100 ml Schlenk flask. This flask was stoppered with a rubber septum and removed from the glove box. The $\text{Ti}(\text{O}-i\text{-C}_3\text{H}_7)_4$ was transferred via a cannula to a triple necked, 500 ml round bottom flask, equipped with a gas inlet and two rubber stoppers. This flask contained 5.931 g (26.69 mmol) *o*-xylene- α,α' -diacetate in 250 ml deoxygenated toluene. The rubber stoppers were replaced, under an argon flush, with a Dean Stark apparatus/condenser and a 500 ml reservoir bulb equipped with a roto-flow teflon stopcock. The



reservoir bulb was charged with 500 ml toluene. The solution was brought to reflux and the distillate was periodically drained from the Dean-Stark apparatus. Simultaneously, toluene was added to the reaction flask to maintain a constant volume. The reflux was continued until the characteristic carbonyl vibration ($\text{C}=\text{O}$) of isopropyl acetate was no longer observed in the infrared spectra of the distillate. The final solution was allowed to cool to room temperature, filtered and the volatiles removed under vacuum yielding 5.945 g (77%) of a soluble, viscous material and 0.130 g (1.7%) of an insoluble white solid on the frit, which was discarded.

^1H NMR: 7.55–6.79 p.p.m. (multiple resonances, 7.11 max), 5.72–4.20 p.p.m. (multiple resonances, 5.24 max), 2.25 p.p.m., and 1.61–0.39 p.p.m. (multiple resonances).

^{13}C NMR: 142–139 p.p.m. (multiple resonances), 131–125 p.p.m. (multiple resonances), 79–70 p.p.m. (multiple resonances), 27–25 (multiple resonances), and 21.3 p.p.m.

Infrared: 2968, 2865, 1457, 1365, 1328, 1214, 1092 (br), shoulder at 1160, 1006 (br), shoulder at 950, 848, 810, 777, 736, 680, 668, 626, and 616 cm^{-1} .

Elemental: (theoretical) Ti, 15.49%; C, 55.70%; H, 7.41%; O, 21.40%.

Analysis: (observed) Ti, 14.44%; C, 58.85%; H, 6.91%; O, 19.80%.

3. Results and discussion

3.1. Synthesis and characterization of the polymeric titanates

The transesterification reaction of titanium isopropoxide that lead to the formation of the polymeric titanate is shown below. The reaction was forced to completion through the removal of isopropyl acetate by distillation. The reaction was stopped when the carbonyl peak of isopropyl acetate (1640 cm^{-1}) was no longer observed in the infrared spectra of the reaction's distillate. The reaction yielded 77 wt % of a soluble viscous polymer and 1.7 wt % of an insoluble product that was discarded. The weight loss (21%) is assumed to be due to the distillation of the alkoxide precursor during the reaction, unrecovered product adhering to the reaction vessel and due to the loss of low molecular weight components during vacuum distillation of the solvent.

Characterization of the polymer was conducted using ^1H NMR, ^{13}C NMR and infrared spectroscopic analyses combined with elemental analysis. The spectroscopic data support the proposed polymer structure shown in Fig. 1. Characteristic infrared peaks and ^1H and ^{13}C NMR resonance peaks confirm the presence of both unreacted titanium isopropoxide ligands and bridging oxy-*o*-xylene groups [13, 14]. The presence of terminal acetate groups is also indicated in the ^1H and ^{13}C NMR spectra (Table II).

The ^1H NMR spectroscopic results were used to estimate quantitatively an average molecular weight (MW_{AV}) for the polymeric titanate. This estimate is based upon the proposed polymer structure and upon

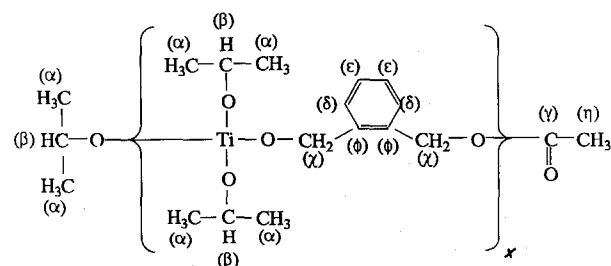


Figure 1 Proposed structure of the polymeric titanate. ($x \approx 15$, $\text{MW}_{\text{av}} \approx 4636\text{ g mol}^{-1}$.)

TABLE II Assigned resonance peaks for ^1H and ^{13}C NMR spectroscopic analysis of the polymeric titanate

Bond assignment	^1H NMR (p.p.m.)	^{13}C CP-MAS-NMR (p.p.m.)	Integration of ^1H NMR	Theoretical integration ($x = 15$)
α	1.61–0.39 (1.14 max)	27–25	61.50	62.00
$\beta + \chi$	5.72–4.20 (5.24 max)	79–70	25.10	30.33
$\delta + \epsilon$	7.55–6.79 (7.11 max)	131–125	20.90	20.00
ϕ	—	142–139	—	—
η	2.25	21.30	1.00	1.00

integration of the ^1H NMR signal intensities. The integration of the ^1H NMR peaks was used to estimate the ratio of bridging oxy-*o*-xylene groups to terminal η groups. The normalized integration results for the peaks represented by $(\delta + \epsilon)$, $(\beta + \chi)$, η and α were calculated as 20.9, 25.1, 1.00 and 61.5, respectively. Based upon the proposed linear polymer structure and an estimated repeat factor of 15.0, the respective theoretical areas would be: 20.00, 30.33, 1.00 and 62.00. This estimate corresponds to an average molecular weight (MW_{AV}) of approximately 4636 g mol^{-1} .

3.2. Characterization of the structural transformations during pyrolysis

The structural changes that occurred in the polymeric titanate during inert atmosphere pyrolysis were studied using thermoanalytical and spectroscopic techniques. The DTA results suggest that two significant reactions occur during pyrolysis (Fig. 2).

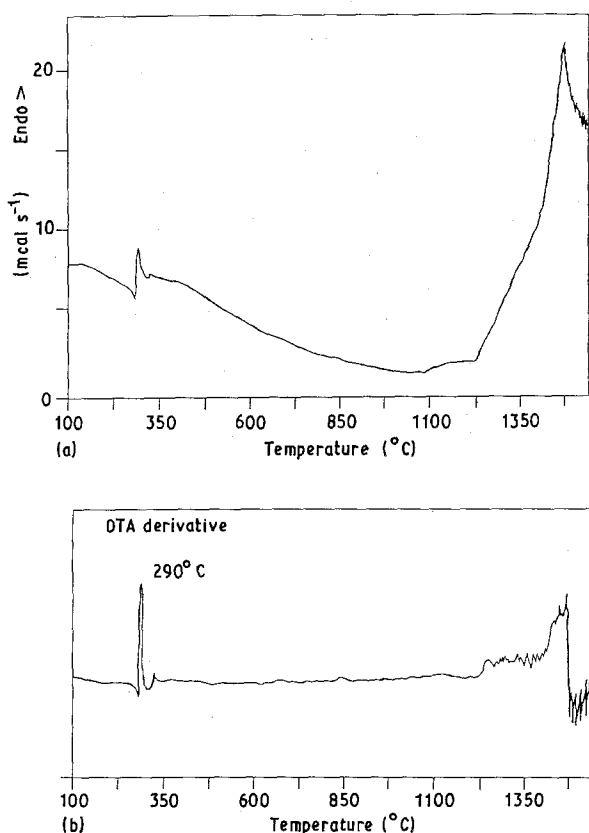


Figure 2 (a) Differential thermal analysis (DTA) of the polymeric titanate, and (b) its derivative. ($5^{\circ}\text{C min}^{-1}$, N_2 atmosphere.)

The derivation of the DTA results indicates that the first exothermic reaction occurs at approximately 290°C (Fig. 2b). The TGA results, presented in Fig. 3, show that this reaction involves a significant weight loss of 60%. Elemental analysis, presented in Table III, shows that this weight reduction was due to the loss of carbon, hydrogen and oxygen.

An infrared spectroscopic analysis of the polymeric titanate during pyrolysis is presented in Fig. 4. A relative reduction in the intensities of the characteristic isopropoxy and bridging *o*-xylene bonding vibrations was observed after pyrolysis at 180°C . After a 4 h isothermal pyrolysis at 300°C , these characteristic peaks were no longer observed in the infrared spectra.

The ^{13}C CP-MAS-NMR spectra indicate a similar reduction in C–O bonding through the loss of the isopropoxy and the bridging oxy-*o*-xylene constituents (Fig. 5). The characteristic resonance peaks for these bonding constituents are still observed in the ^{13}C CP-MAS-NMR spectra after a 4 h isothermal pyrolysis at 180°C . However, these resonance peaks are no longer detected after pyrolysis at 360°C . In this spectrum, the majority of peaks are due to the aromatic carbon resonances of the δ , ϵ and ϕ environments and their spinning side bands. Remaining resonance peaks at 39 and 20 p.p.m., suggest the

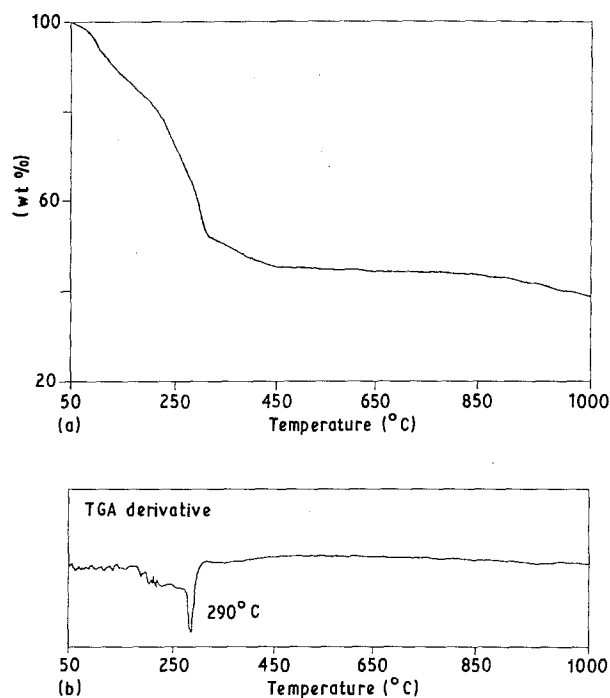


Figure 3 (a) Thermal gravimetric analysis (TGA) of the polymeric titanate, and (b) its derivative. ($5^{\circ}\text{C min}^{-1}$, N_2 atmosphere.)

TABLE III Elemental analysis of the polymeric titanate after inert atmosphere pyrolysis (4 h isothermal)

Temperature (°C)	Titanium		Carbon		Hydrogen		Oxygen	
	Wt %	Molar ratio	Wt %	Molar ratio	Wt %	Molar ratio	Wt %	Molar ratio
Polymer	14.44	1.00	58.85	16.28	6.91	22.92	19.80	4.11
180	15.60	1.00	56.53	14.46	4.46	13.69	23.41	4.48
360	31.58	1.00	42.17	5.32	1.83	2.76	24.42	2.32
700	32.30	1.00	42.85	5.21	< 0.5	< 0.74	24.85	2.30
1200	52.53	1.00	38.32	2.91	< 0.5	< 0.46	8.60	0.49
1500	57.99	1.00	38.94	2.68	< 0.5	< 0.41	3.07	0.16

* Oxygen wt % determined from the experimental residue.

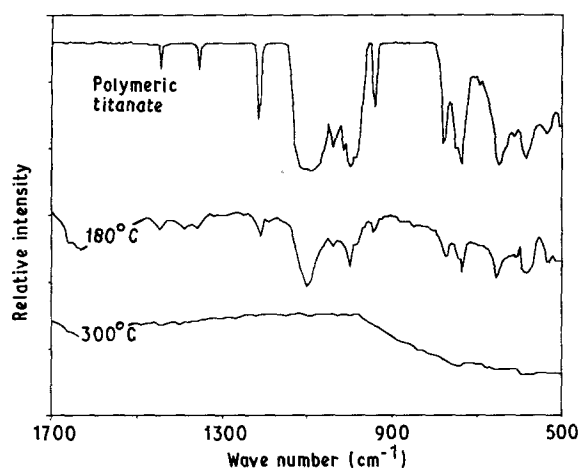


Figure 4 Infrared spectroscopic analysis of the polymeric titanate during inert atmosphere pyrolysis. (4 h isothermal.)

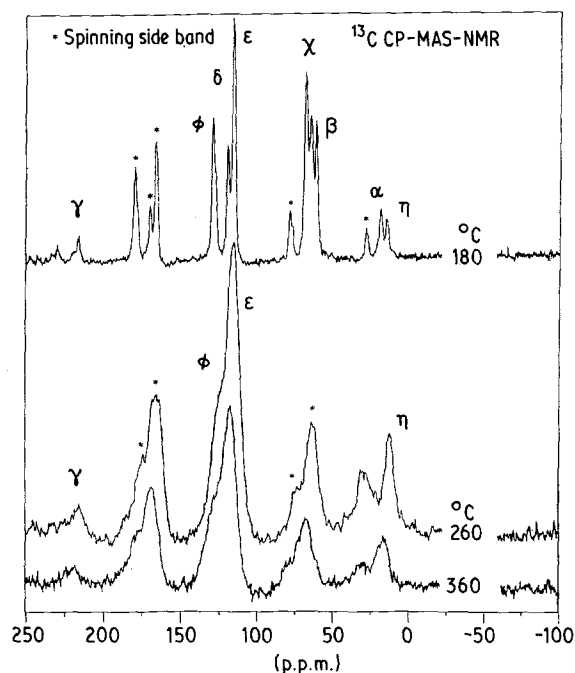


Figure 5 ^{13}C CP-MAS-NMR analysis of the polymeric titanate during inert atmosphere pyrolysis.

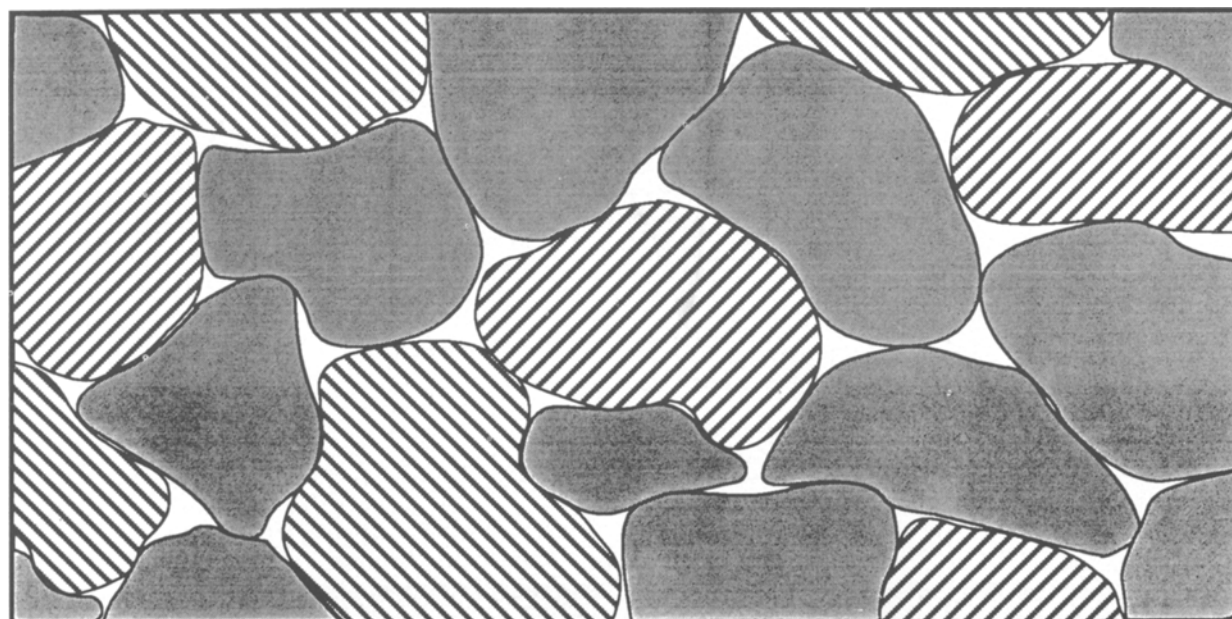
presence of unreacted acetate ligands (20 p.p.m.) and hydrocarbon fragments. The existence of hydrocarbon fragments is supported by the aromatic resonance peaks and the peak at 39 p.p.m. that describes cross-linked $-\text{CH}_2-$ (e.g. $\text{C}_6\text{H}_4-\text{CH}_2-\text{C}_6\text{H}_4-$) carbon environments.

According to the experimental data, the exothermic reactions that occurred during low-temperature pyrolysis to 300°C involved the destruction of the titanium alkoxy constituents ($\text{Ti}-\text{O}-\text{C}$). The loss of organic by-products during the reaction would explain the dramatic weight loss of carbon, hydrogen and oxygen. The destruction of the alkoxy bonds is proposed to result in the formation of an amorphous titanium oxide network with intimately dispersed hydrocarbon fragments (Fig. 6). This proposal is supported by the eventual crystallization of TiO_2 anatase and by the aromatic carbon resonance peaks observed in the ^{13}C CP-MAS-NMR spectra. The crystalline anatase phase was detected in the XRD results after pyrolysis at 500°C (Fig. 7). Based on a Scherrer diffraction peak broadening analysis, an average TiO_2 crystal diameter of 4 nm was estimated [15]. This value can be used as an upper limit for the size of the amorphous titania particles proposed in Fig. 6.

According to the XRD results, the TiO_2 anatase phase is stable during further pyrolysis to 700°C . However, after a 4 h isothermal pyrolysis at 800°C , the XRD results indicate the presence of crystalline TiO_2 rutile and carbon-deficient TiC_x ($x < 1$). The carbon deficiency of the TiC_x crystalline phase was indicated by the shift of the characteristic TiC diffraction peaks to higher angles (Fig. 7) [4]. The broad diffraction peaks in this spectrum suggest that both the TiO_2 rutile and the TiC_x crystallites are extremely small.

Isothermal pyrolysis for 4 h at elevated temperatures of 900 and 1000°C caused no significant changes in the XRD spectra. However, after a 4 h isothermal pyrolysis at 1100°C , the XRD results only indicate the presence of carbon deficient TiC_x . The formation of TiC_x at these temperatures was unexpected because the DTA results did not indicate a reaction until approximately 1225°C . Because TiC_x was detected after pyrolysis at lower temperatures, it can be inferred that its formation is both temperature and time dependent. This suggests that longer isothermal heat treatments may enable the formation of pure TiC_x ceramics at lower temperatures (800 – 1000°C).

The formation of TiC_x obviously involved the carbothermal reduction of the titanium oxide constituents. Elemental analysis indicated that the loss of carbon and oxygen occurred at a molar ratio of approximately 1:1 between 700 and 1500°C . This suggests that the carbothermal reduction of the oxide



5 nm

- Intimately dispersed, amorphous carbon particles. It is proposed that these particles are formed by the agglomeration of the hydrocarbon fragments following the destruction of the titanium alkoxy bonds.

- Amorphous titania particles that form after the destruction of the titanium alkoxy bonds. After pyrolysis at temperatures exceeding 500°C, these particles crystallize into TiO₂ anatase with an approximate average crystal diameter of 4 nm.

Figure 6 Proposed morphology of polymeric titanate after inert atmosphere pyrolysis at temperatures exceeding 290 °C.

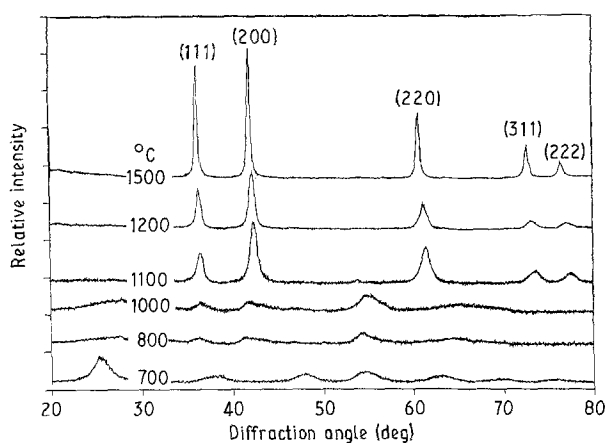


Figure 7 XRD analysis of the polymeric titanate during inert atmosphere pyrolysis. (4 h isothermal.)

constituents occurred through the formation of carbon monoxide gas.

The lack of stoichiometry in the TiC_x crystal phase was not due to a lack of carbon because elemental analysis indicated that a large excess of carbon exists in the samples. It is assumed that the excess carbon is located at the TiC_x grain boundaries as carbon inclusions and that not enough thermal energy was supplied to allow for the required diffusion of carbon into the crystal structure.

According to the binary phase diagram of titanium and carbon [16], crystalline TiC_x can exist with a

carbon concentration ranging between 1.00 and 0.32. The concentration of carbon in the crystal structure can be estimated from the cubic lattice parameter, a_0 [4]. The carbon concentrations in the TiC crystals after pyrolysis at various temperatures and for different isothermal holding times are estimated in Table IV. The results clearly indicate that pyrolysis at elevated temperatures and for longer isotherms enables more carbon to diffuse into the crystalline phase, thereby resulting in a better proportioned TiC crystal.

3.3. Exploratory preparation and characterization of TiC fibres and thin films

The polymeric titanate exhibited rheological properties that allowed for the formation of fibres and thin films which could be thermally converted into TiC. In the following section, the preparation and the properties of these fibres and films are discussed.

3.4. Preparation and analysis of TiC fibres

Hand-drawn fibres were obtained directly from the polymeric titanate. These fibres were cured at 80 °C for approximately 20 h and then slowly pyrolysed to temperatures between 500 and 1500 °C. Pyrolysis at 1500 °C resulted in the formation of a crystalline TiC fibre.

TABLE IV Summary of the XRD results for the polymeric titanate pyrolysed at various temperatures

Temp. (°C)	Time (h)	Crystal structure	TiC lattice parameter (nm)	Crystal stoichiometry	Crystal size (nm)
300	4	Amorphous	—	—	—
500	4	TiO ₂ anatase—distorted cubic close-packed	—	—	4
700	4	TiO ₂ anatase—distorted cubic close-packed	—	—	4.8
800	4	TiO ₂ rutile + TiC	$a = 0.4260$	$x < 0.40$	5.0 + 6.0
900	4	TiO ₂ rutile + TiC	$a = 0.4261$	$x < 0.40$	5.2 + 6.4
1000	4	TiO ₂ rutile + TiC	$a = 0.4265$	$x < 0.40$	5.4 + 7.4
1100	4	TiC, cubic close-packed	$a = 0.4261$	$x < 0.40$	11
1200	1	TiC, cubic close-packed	$a = 0.4265$	$x < 0.40$	6.8
	4	TiC, cubic close-packed	$a = 0.4281$	TiC _{0.41}	15
1500	1	TiC, cubic close-packed	$a = 0.4278$	TiC _{0.41}	7.4
	2	TiC, cubic close-packed	$a = 0.4287$	TiC _{0.42}	18
	4	TiC, cubic close-packed	$a = 0.4313$	TiC _{0.60}	30

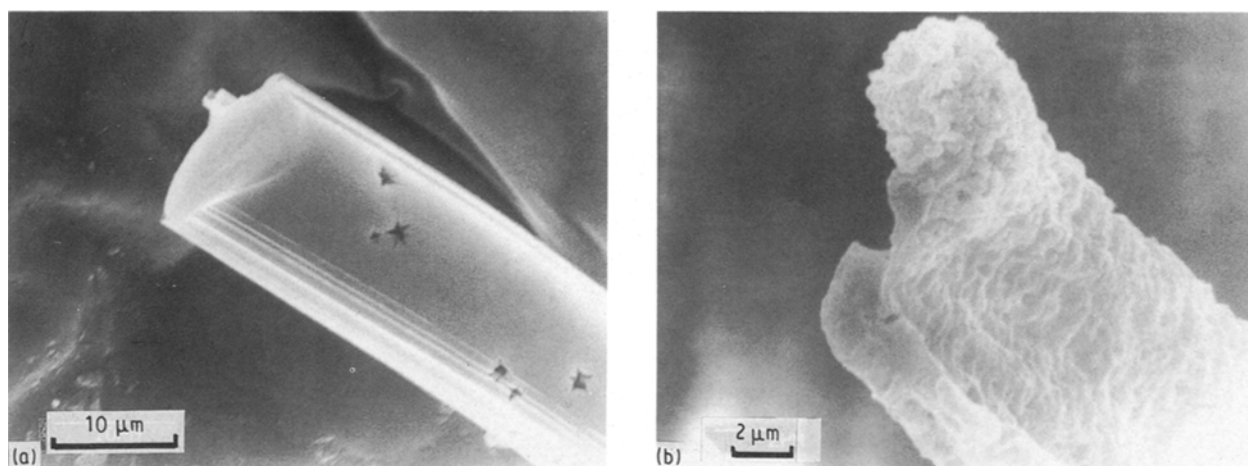


Figure 8 Scanning electron microscopic (SEM) analysis of the fibres prepared from the polymeric titanate: (a) 500 °C 4 h; (b) 1500 °C, 4 h.

The quality of the TiC fibres prepared from the polymeric titanate was investigated using scanning electron microscopy (SEM). A comparison between a fibre pyrolysed at 500 and at 1500 °C is presented in Fig. 8. The fibre pyrolysed at 500 °C exhibits a smooth, slightly porous surface morphology. The microstructure of this fibre is assumed to include small crystallites of TiO₂ anatase and intimately dispersed hydrocarbon fragments. The fibre pyrolysed at 1500 °C, exhibits a highly porous surface that is principally composed of TiC crystallites. The porosity observed in these fibres is a direct result of the large weight loss that occurs during pyrolysis.

The TiC fibres prepared from the polymeric titanate are very brittle and difficult to handle. It is likely that this mechanical behaviour is due to the influence of the large number of pores. A pore in a fibre acts as a stress concentration site and the extreme porosity observed in these fibres would explain their lack of mechanical strength.

3.5. Preparation and analysis of TiC thin films

Thin films were prepared by dipping fused quartz or single-crystal silicon substrates into a dilute solution of the polymeric titanate. In our experiments, films of varying thickness were obtained by controlling the

substrate dipping speed into a 10 wt % *n*-hexane solution. Dipping speeds ranging between 1 and 4 in min⁻¹ (~ 2.5 and 10 cm min⁻¹) were used. The films were cured at 80 °C for approximately 20 h before high-temperature pyrolysis.

Ellipsometry and scanning electron microscopy were used to study the thickness and the morphology of the dip-coated films. Films were prepared that varied in thickness from several tens to a few hundred nanometres depending upon the processing conditions. Films of 30 and 100 nm were prepared by single-dip processing at 4 and 1 in min⁻¹ (~ 10 and 2.5 cm min⁻¹), respectively. Scanning electron micrographs indicated that the film surfaces were free of cracks and pores even after inert atmosphere pyrolysis at 1000 °C (Fig. 9). The lack of pores is due to the strong adhesion bonding of the film and substrate. This bonding limits densification and viscous material flow directionally towards the film–substrate interface.

The d.c. electrical conductivities of the thin films were analysed at temperatures between 25 and 500 °C using Seebeck and four-point probe techniques. The results indicate that the films pyrolysed at 500, 700 and 900 °C behave as n-type semi-conductors with room-temperature d.c. conductivities of 0.04, 0.80 and 85.0 Ω⁻¹ cm⁻¹, respectively (Fig. 10).

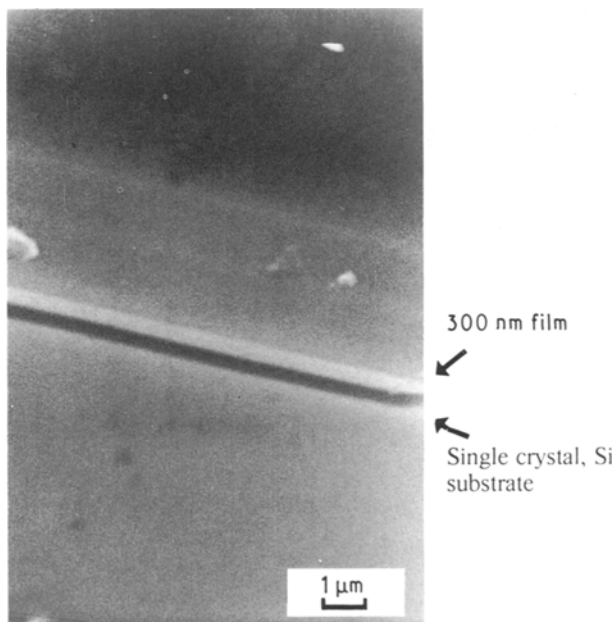


Figure 9 Cross-sectional scanning electron micrograph of a multi-dipped thin film prepared from the polymeric titanate and pyrolysed at 1000 °C for 4 h.

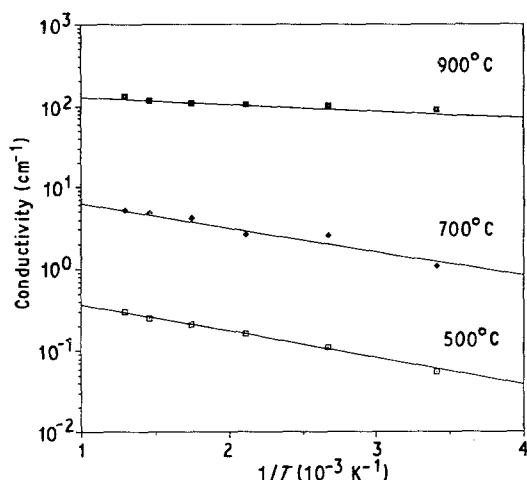


Figure 10 Conductivity behaviour of the films prepared from the polymeric titanate after 4 h isothermal pyrolysis at 500, 700 and 900 °C.

The microstructures of the films pyrolysed at 500 and 700 °C are characterized by small crystallites of TiO₂ anatase and intimately dispersed hydrocarbon fragments. Either phase could be responsible for the conductivity behaviour of the films. However, it is unlikely that the conductivity is due to the intimately dispersed hydrocarbon inclusions because carbon is essentially a metallic conductor ($\sigma_{0^\circ\text{C}} = 750 \Omega^{-1} \text{cm}^{-1}$) [1]. If carbon was responsible for the electrical behaviour of the films, larger conductivity values would have been expected. Also, because carbon is a metallic conductor, its conductivity would be expected to decrease with increasing temperature. For these reasons, it is assumed that the electrical behaviour is due to conduction in the oxide phase. TiO₂ anatase is an insulator ($\sigma_{30^\circ\text{C}} = 25 \mu\Omega^{-1} \text{cm}^{-1}$) [1], but it does behave as an n-type semi-conductor if it is oxygen deficient [17].

The conductivity behaviour of the film pyrolysed at 900 °C is also thought to be due to oxygen-deficient TiO_{2-x} conduction. The microstructure of the film pyrolysed at 900 °C includes intimately dispersed carbon inclusions and small crystallites of TiO₂ rutile and TiC_x. Because both carbon and TiC are essentially metallic conductors [$\sigma(\text{TiC})_{30^\circ\text{C}} = 5000 \Omega^{-1} \text{cm}^{-1}$], it is again assumed that the n-type semiconductor behaviour of the film is due to oxygen deficient TiO_{2-x} conduction [17].

4. Conclusions

Transesterification of titanium isopropoxide with *o*-xylene- α,α' -diacetate has been successfully employed in the preparation of a polymeric titanate that can be used for the production of TiC. During inert atmosphere pyrolysis at approximately 290 °C, this polymeric titanate decomposes into an amorphous titania network with intimately dispersed, hydrocarbon fragments. The amorphous titania particles are assumed to have an average diameter of approximately 4 nm. Further pyrolysis involves the crystallization of TiO₂ anatase at 500 °C. Isothermal pyrolysis for 4 h at 800 °C involves the formation of crystalline TiO₂ rutile and carbon-deficient TiC_x. After a 4 h isothermal pyrolysis at 1100 °C, only carbon-deficient TiC_x is detected. Pyrolysis at higher temperatures and for longer isotherms improves the internal ratio of titanium and carbon in this crystal phase.

The physical and rheological properties of the polymeric titanate enabled the formation of fibres and thin films. The fibres are porous and brittle. The porosity is due to the large weight losses that occur during pyrolysis and the brittleness is due to the stress concentrations caused by the pores. Thin films were easily obtained from the polymeric titanate and they were free of surface cracks and pores even after pyrolysis at 1000 °C. The films pyrolysed at 500, 700 and 900 °C behave as n-type semi-conductors and exhibit room-temperature d.c. conductivities of 0.04, 0.80 and 85.0 $\Omega^{-1} \text{cm}^{-1}$, respectively.

Acknowledgement

The authors are grateful to the National Science Foundation for financial support of this research through contract grant DMR-87-06379.

References

1. D. W. RICHERSON, "Modern Ceramic Engineering" (Marcel Dekker, New York, 1982) pp. 72, 93.
2. V. S. NESHPOR, V. P. NIKITIN and V. I. NOVIKOV, *Izvest. Akad. Nauk SSSR* 7 (1971) 1643.
3. G. S. GIROLAMI, J. A. JENSEN and D. M. POLLINA, *J. Amer. Chem. Soc.* 109 (1987) 1579.
4. E. K. STORM, "The Refractory Carbides" (Academic Press, New York, 1967) Ch. 1.
5. S. YAJIMA, Y. HASEGAWAW, K. OKAMURA and T. MATSUZAWA, *Nature* 273 (1978) 525.
6. K. J. WYNNE and R. W. RICE, *Ann. Rev. Mater. Sci.* 14 (1984) 297.
7. R. W. WEST, "Ultrastructure Processing of Ceramics, Glasses and Composites", edited by L. L. Hench and D. R. Ulrich (Wiley, New York, 1984) p. 19.

8. R. R. WILLIS, R. A. MARKLE and S. P. MUKHERJEE, *Amer. Ceram. Soc. Bull.* **62** (1983) 904.
9. S. J. TING, C. J. CHU, E. LIIMATTA, J. D. MACKENZIE, T. GETMAN and M. F. HAWTHORNE, in "Better Ceramics Through Chemistry IV", MRS Conference Proceedings, 16-20 April 1990, San Francisco, CA, to be published.
10. D. C. BRADLEY, R. C. MEHROTRA and D. P. GAUR, "Metal Alkoxides" (Academic Press, New York, 1978).
11. D. C. BRADLEY, *Adv. Inorg. Chem. Radiochem.* **15** (1972) 259.
12. R. F. NYSTROM and W. G. BROWN, *J. Amer. Chem. Soc.* **69** (1947) 1198.
13. T. W. SOLOMANS, "Organic Chemistry" (Wiley, New York, 1976).
14. E. D. BECKER, "High Resolution NMR" (Academic Press, San Diego, 1980).
15. B. D. CULLITY, "Elements of X-ray Diffraction" (Addison-Wesley, Menlo Park, CA, 1978) p. 99.
16. B. UHRENIUS, *CALPHAD* **8** (2) (1984) 101.
17. W. D. KINGERY, "Introduction to Ceramics" (Wiley, New York, 1976).

*Received 19 April
and accepted 5 August 1991*